Journal of Wind Engineering and Industrial Aerodynamics, 7 (1981) 273—287

AN APPROACH TO THE DETERMINATION OF WIND LOAD EFFECTS ON LOW-RISE BUILDINGS

J.D. HOLMES and R.J. BEST

Department of Civil and Systems Engineering, James Cook University of North Queensland, Townsville, Queensland 4811 (Australia)

(Accepted in revised form October 10, 1980)

Summary

A covariance integration method for the determination of fluctuating overall structural loads due to wind and their effects on low-rise buildings is described. The required aerodynamic information can be obtained from boundary-layer wind tunnel tests; static structural-influence coefficients are also required. The method is an alternative to the direct on-line weighting technique, but is less demanding on wind tunnel instrumentation and data acquisition facilities. To obtain peak values, Gaussian probability distributions have been assumed for the loads or their effects.

Use of the method is demonstrated by calculations of gust factors and peak values for various structural loads on the central bay of a single-storey house, using aerodynamic data obtained from a 1/50-scale wind tunnel model.

Notation

A	area
C_p	pressure coefficient
D	drag
F_u	factor in empirical expression for turbulence intensity (see Fig. 3)
g	peak factor
G	gust factor
h	eaves height of building
i, j	panel numbers
L	lift
M	moment
n	frequency
N	number of panels
p	pressure
r	correlation coefficient
S	spectral density (see Fig. 4)
t	time
T	time period

u longitudinal velocity
V_1, V_2 hold-down forces for roof truss
z height
z_0 roughness length
z_r reference height (see Fig. 3)
ΔA panel area
β influence coefficient
γ Euler's constant (0.5772)
η arbitrary structural effect
λ peak wavelength of spectrum (see Fig. 4)
ν cycling rate (see eqn. (6))
ρ air density

Superscripts:

$\bar{}$ mean value
$'$ fluctuating value
$\hat{}$ maximum value
$\check{}$ minimum value
$\cdot$ time derivative

Matrices:

$[\Delta A]$ diagonal matrix of panel areas
$[C_p']$ diagonal matrix of r.m.s. pressure coefficients
$[\dot{C}_p']$ diagonal matrix of r.m.s. pressure-derivative coefficients
$\{\beta\}$ column vector of influence coefficients
$\{\beta\}^T$ row vector of influence coefficients
$[r]$ square matrix of pressure correlation coefficients
$[\dot{r}]$ square matrix of pressure-derivative correlation coefficients

The superscript ^{T} indicates transpose matrices.

1. Introduction

Low-rise buildings, which represent a high percentage of engineer-designed structures, have traditionally been designed for wind loads by using simplified Code procedures. These amount, in the case of many Codes and Standards (e.g., refs. 1 and 2), to the use of a peak-gust design wind-speed, together with single-valued pressure coefficients. There are strong arguments for continuing this method in Code form, on the basis of its ease of application. However, the approach generally leads to conservative designs for global loads and their effects on larger low-rise structures. This is because of the difficulty in taking account of the effects of fluctuating pressures at different

parts of the exposed building surface, which are only partially correlated with each other. The fluctuating pressures arise from upwind turbulent velocity fluctuations (which are intense at the heights associated with low buildings), from unsteady pressures generated in the separated flow regions by the structure itself, or by interaction between these two processes.

In a recent comprehensive wind tunnel study of low-rise buildings carried out at the University of Western Ontario [3,4], an attempt was made to define more closely the fluctuating wind-induced responses or effects, as well as the point pressures or loads over small areas, by means of a complex measurement system. This procedure involved two separate stages:

(i) "pneumatic averaging" (see Sections 3.1 and 3.2) of point pressures over panels tributary to wall girts and roof purlins;

(ii) numerical on-line weighting using appropriate influence lines, to determine instantaneous values of such responses as total uplift and frame-bending moments, applicable to a single bay. Estimates of the required statistical properties of these parameters were then obtained from sample records.

In the study, the fluctuating values of structural *effects* of interest to designers were obtained directly, and, implicitly, full account was taken of the effects of partial correlation of the fluctuating loads across a building.

However, there are a number of disadvantages in the procedure, as follows:

(i) a large number of pressure transducers are required to be operating simultaneously;

(ii) simultaneous sampling of ten or more input channels and multiplication by the appropriate influence factors at a suitable rate may be beyond the capabilities of many computer systems associated with wind tunnels;

(iii) if it is necessary to monitor further structural effects, further wind tunnel tests are required, unless the unweighted panel load records are stored.

It is the purpose of the present paper to describe an alternative procedure, based on *covariance integration*, for obtaining fluctuating and peak values of structural effects. The wind tunnel test data required can be obtained relatively easily with only two pressure transducers and two data channels. Discussion of the basis for the procedure is followed by the calculation of loads on the central bay of a domestic house in rural terrain, using aerodynamic data from a 1/50-scale model tested in a boundary-layer wind tunnel.

2. Basis of the covariance integration method

2.1 Mean square of fluctuating responses

The pressures acting on the surface of a building are assumed to be stationary and ergodic random processes. This will be close to the real situation when the mean velocity, $\bar{u}$, can be assumed to be constant over a period such as ten minutes during the passage of a wind storm.

It is shown in the Appendix, using standard averaging procedures, that the root-mean-square of the fluctuating value of any structural effect, η, is related

in the following way to the loads on N individual panels exposed to wind pressures:

$$(\overline{\eta'^2})^{1/2} = \left(\sum_{i=1}^{N} \sum_{j=1}^{N} \overline{p_i' p_j'} \, \beta_i \, \beta_j \, \Delta A_i \, \Delta A_j \right)^{1/2} \tag{1}$$

Here, β_i and β_j are the structural influence coefficients associated with the panels i and j of areas ΔA_i and ΔA_j, respectively. The β's may be obtained by standard static structural-analysis procedures. $\overline{p_i' p_j'}$ is the *covariance* between the fluctuating wind pressures $p_i(t)$ and $p_j(t)$ acting on the panels i and j, respectively. For all the N i's and N j's, there are a total of N^2 values of this quantity, giving a symmetric square matrix — the covariance matrix. This matrix, which may be obtained from wind tunnel tests, is the key to the method, as it contains all the required information on the statistical correlation between the fluctuating panel loads over the building for a particular wind direction.

It should be noted that the derivation of eqn. (1) neglects any resonant dynamic effects, an assumption which is normally valid for low-rise structures. This assumption means that information on the auto- and cross-spectral densities for point pressures and panel loads, which is required for calculation of the response of tall buildings and other flexible structures to wind, is not required in this case.

If the number of panels, N, influencing a particular structural parameter can be limited to a manageable number, and the required covariance matrix obtained from wind tunnel tests, then the double summation in eqn. (1) can be carried out using simple computer or pocket calculator programs.

The covariance term in eqn. (1) is often more conveniently written in the form of a product of the r.m.s. fluctuating-pressure coefficients C'_{pi} and C'_{pj}, the non-dimensional *cross-correlation* coefficient r_{ij}, and the dynamic pressure:

$$\overline{p_i' p_j'} = (\tfrac{1}{2} \rho \bar{u}^2)^2 \, C'_{pi} \, C'_{pj} \, r_{ij} \tag{2}$$

Then eqn. (1) becomes

$$(\overline{\eta'^2})^{1/2} = \tfrac{1}{2} \rho \bar{u}^2 \left(\sum_{i=1}^{N} \sum_{j=1}^{N} r_{ij} \, C'_{pi} \, C'_{pj} \, \beta_i \, \beta_j \, \Delta A_i \, \Delta A_j \right)^{1/2} \tag{3}$$

For computer programming, it may be more convenient to re-state eqn. (3) in matrix form:

$$(\overline{\eta'^2})/\tfrac{1}{2} \rho \bar{u}^2 = (\{\beta\}^T \, [\Delta A] \, [C'_p] \, [r] \, [C'_p] \, [\Delta A] \, \{\beta\})^{1/2} \tag{4}$$

The matrix terms in eqn. (4) are defined at the beginning of this paper (see Notation).

2.2 Peak responses

More relevant for design purposes is the peak value $\hat{\eta}$ of the structural parameter over a specified time period T. This peak value is itself a random value, but its probability distribution is relatively narrow, and it has become common to consider only the average peak value over the specified time period T.

It has been shown by Cartwright and Longuet-Higgins [5] and Davenport [6] that the average largest value of a *Gaussian* or normally distributed random process in a time period T is given by

$$\bar{\hat{\eta}} = \bar{\eta} + (\overline{\eta'^2})^{1/2} \left(\sqrt{2 \log_e \nu T} + \gamma/\sqrt{2 \log_e \nu T}\right) \tag{5}$$

where γ is Euler's constant (0.5772) and ν is the *cycling rate* for the response $\eta(t)$, given by

$$\nu = (\overline{\dot{\eta}'^2})^{1/2}/2\pi(\overline{\eta'^2})^{1/2} \tag{6}$$

where $(\overline{\dot{\eta}'^2})^{1/2}$ is the root-mean-square value of the *derivative* of $\eta(t)$. By a process analogous to that used in the Appendix to derive eqn. (1), it can readily be shown that:

$$(\overline{\eta'^2})^{1/2} = \left(\sum_{i=1}^{N} \sum_{j=1}^{N} \overline{\dot{p}_i' \dot{p}_j'}\, \beta_i\, \beta_j\, \Delta A_i\, \Delta A_j\right)^{1/2}$$

$$= \tfrac{1}{2}\rho \bar{u}^2 \left(\sum_{i=1}^{N} \sum_{j=1}^{N} \dot{r}_{ij}\, \dot{C}_{pi}'\, \dot{C}_{pj}'\, \beta_i\, \beta_j\, \Delta A_i\, \Delta A_j\right)^{1/2} \tag{7}$$

where $\dot{C}_{pi}'$ and $\dot{C}_{pj}'$ are the r.m.s. values of dC_{pi}/dt and dC_{pj}/dt respectively, and $\dot{r}_{ij}$ has been used to denote the cross-correlation matrix for the *derivative* of the pressure fluctuations.

Again, re-stating eqn. (7) in matrix form,

$$(\overline{\dot{\eta}'^2})^{1/2}/\tfrac{1}{2}\rho \bar{u}^2 = (\{\beta\}^T\, [\Delta A]\, [\dot{C}_p']\, [\dot{r}]\, [\dot{C}_p']\, [\Delta A]\, \{\beta\})^{1/2} \tag{8}$$

Thus from eqns. (3) or (4), (5), (6), and (7) or (8), the average maximum value of the parameter $\eta(t)$ in the time period T, say ten minutes, can be calculated. Again, the vector $\{\dot{C}_p'\}$ and the matrix $[\dot{r}]$ must be obtained from wind tunnel tests.

The assumption that η has a Gaussian distribution needs further investigation, as it is well known that point-pressure fluctuations, especially in separated flow regions, depart from the Gaussian form at the tails of the distribution. However, for structural effects influenced by pressures over larger areas and with influence coefficients of varying sign, the central-limit theorem will tend to make the probability distributions close to Gaussian. Also, further investigation may enable eqn. (5) to be modified to account for non-Gaussian tails.

3. Aerodynamic measurements on a house

To illustrate the method, some of the necessary aerodynamic data (as indicated in Section 2) were obtained for a house, from a model tested in a boundary-layer wind tunnel. A description of the experimental methods used and of the results follows.

3.1 Experimental

The boundary-layer wind tunnel used for the experiments was of the open-circuit type, having a 2.5 m wide by 2.0 m high cross-section and a 13.5 m long working-section. The tunnel is powered by a 45-kW AC electric motor driving a five-bladed, fixed-pitch, axial-flow fan 2.4 m in diameter, through a five-speed gearbox. The fan is mounted downwind of the test section. A description of the design and performance of the wind tunnel has been given by Holmes [7].

A 1/50-scale model of a tropical-style low-set house, with a 10° pitch gable roof and eaves and verges overhangs, was made from Perspex sheeting. The model dimensions are shown in Fig. 1. Pressures were measured over a central

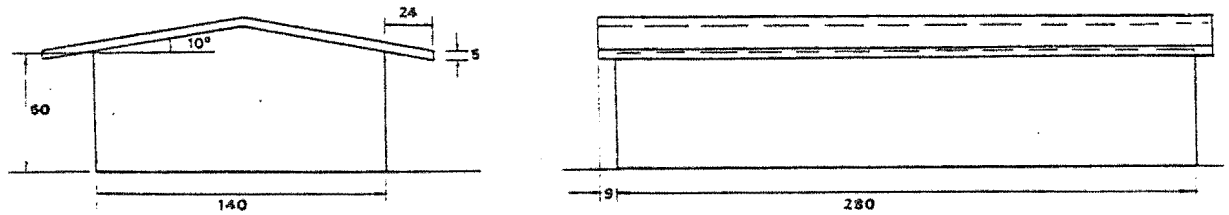

Fig. 1. Dimensions of 1/50-scale house model.

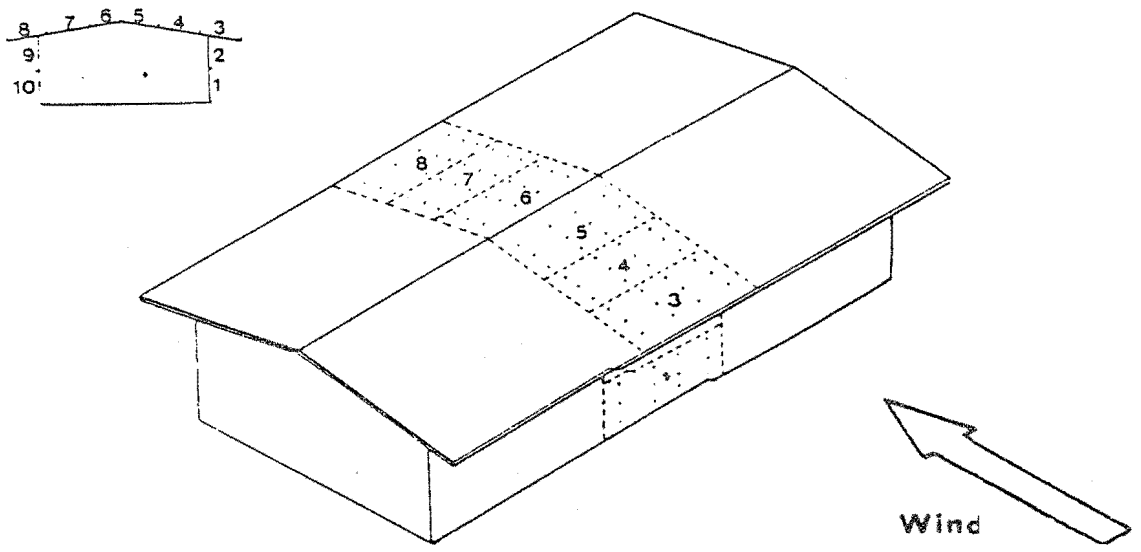

Panels and pressure-tap grids.

band across the model (Fig. 2). This band was divided into ten "panels" each containing twelve pressure taps. The taps consisted of stainless-steel hypodermic tubing fixed into holes drilled into the Perspex roof and walls. Taps from within a single "panel" were connected to a common manifold, which was, in turn, connected to a "Scanivalve" containing a Setra-237 capacitance-type pressure transducer. This technique has been called "pneumatic averaging" (see Section 3.2). Due to a limitation on the manifold connectors available for the present work, not all the twelve pressure taps in each panel were used. For the windward half, panels 1—5 (Fig. 2), 11 pressure taps were used; for the remaining panels, 6—10, 9 pressure taps from the twelve were connected to the manifolds.

Two "Scanivalves" and two transducers were available, thus allowing simultaneous measurement from any two "panels". 50 mm of 1.5 mm internal diameter plastic tubing was used for each of the connections between the pressure taps and the manifolds, and 450 mm of the same tubing for the manifold—"Scanivalve" connection. Two fine-diameter restrictors were inserted partway along the latter tubing, to remove the resonant peak in the frequency response.

Velocity measurements were made with a T.S.I. Type 1054B linearised constant-temperature anemometer, with a hot-film probe. The voltages from both the pressure transducers and the hot-film anemometer were digitised and processed by a PDP8/E minicomputer, which was also used to control which panel was connected to each "Scanivalve".

3.2 Pneumatic averaging

Stathopoulos and Surry [8, 9] have investigated in some depth the use of pneumatic averagers. By spectral measurements using both sinusoidal excitation and wide-band random inputs, they found satisfactory linear response characteristics. The amplitude—frequency response functions obtained were found to differ little from those of each of the component tubes. As the manifold and tube geometries used in the present tests were different from those used by Stathopoulos and Surry, similar frequency response measurements were carried out. Again the measured amplitude—frequency response functions were found to be closely similar to that of a single-tube system with restrictors, i.e., a smooth "roll-off", with a half-power point at about 100 Hz.

A further check on the method was carried out in the present tests, as follows. The mean and fluctuating pressures at each pressure tap within panels 3 and 4 were measured separately, together with all the cross-correlations between the individual taps. Using the same techniques as those described in Section 2, the mean, r.m.s. and correlation coefficients for the loads and their derivatives on the two panels were computed and compared with values obtained from the pneumatic averaging procedure. The basic pressure coefficients obtained from the pneumatic averaging were about 10% lower than those computed from the individual taps — this bias probably could be attributed, at least in part, to errors in the reference velocity used to compute the coef-

ficients. However, encouraging agreement was found between the non-dimensional correlation coefficients: r_{34} was measured as 0.69 for the pneumatically averaged panel pressures, compared with a computed value of 0.67 from the individual tap results.

Although further checking of the pneumatic averaging method is desirable, the technique, at present, appears to be sound enough to justify its use for carrying out primary averaging of point pressures.

3.3 Boundary layer simulation

The lower part of a 1/50-scale rural atmospheric boundary layer was simulated in the wind tunnel by using a 300 mm high plain barrier or fence at the start of the test section, together with carpet covering the floor upwind of the model. The resulting mean velocity and turbulence intensity profiles compare well with standard data based on full-scale measurements, with a roughness length of 35 mm (Fig. 3).

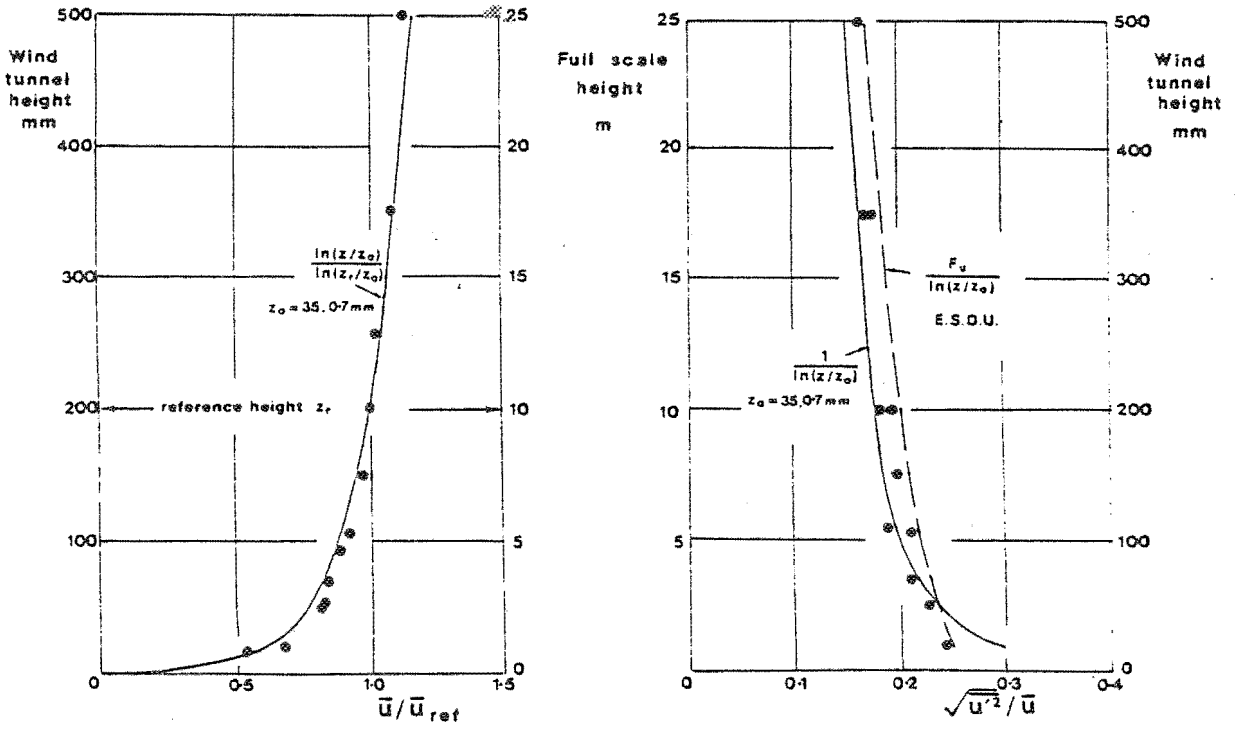

Fig. 3. Mean velocity and turbulence intensity profiles.

The longitudinal-turbulence spectrum is shown in Fig. 4, compared with the von Karman—Harris spectrum, with a length scale derived from that suggested by the Engineering Sciences Data Unit [10], for the roughness length of 35 mm. The wind tunnel spectrum is shifted to the high-frequency side by a factor of about two. However, the turbulence scales are much larger than the dimensions of the model, and this shift is not believed to have a significant effect on the measured pressure.

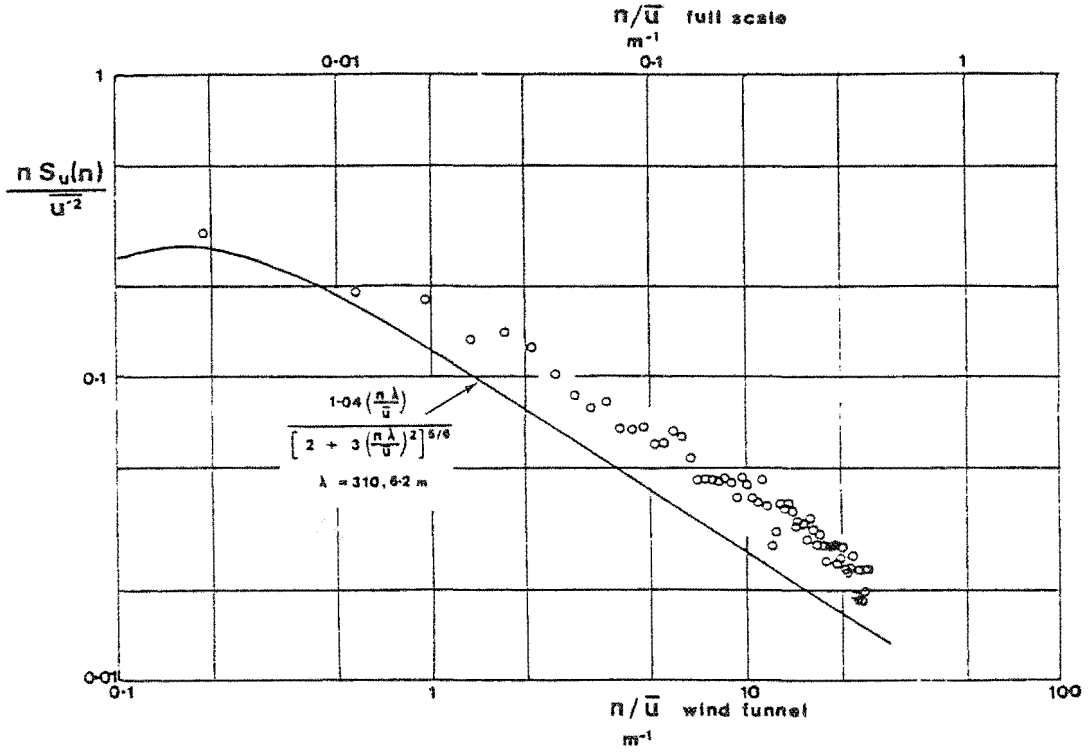

Fig. 4. Longitudinal turbulence spectrum at eaves height.

3.4 Results

For each panel on the model, the mean, r.m.s. and peak pressure coefficients were measured. These are defined conventionally as follows:

$$\overline{C}_p = (\overline{p} - p_{ref})/\tfrac{1}{2}\rho\bar{u}_h^2 \tag{9}$$

$$C'_p = (\overline{p'^2})^{1/2}/\tfrac{1}{2}\rho\bar{u}_h^2 \tag{10}$$

$$\hat{C}_p = (\hat{p} - p_{ref})/\tfrac{1}{2}\rho\bar{u}_h^2 \tag{11}$$

$$\check{C}_p = (\check{p} - p_{ref})/\tfrac{1}{2}\rho\bar{u}_h^2 \tag{12}$$

The reference static pressure p_{ref} and the velocity $\bar{u}_h$ were both measured at, or corrected to, the eaves height of the house. The peak pressures $\hat{p}$ and $\check{p}$ are for a full-scale time period of about 10 minutes. In addition, the r.m.s. value of the coefficient of rate of change of pressure, $\dot{C}'_p$, was also computed. This can be expressed in non-dimensional form as follows:

$$h\dot{C}'_p/\bar{u}_h = (\overline{\dot{p}'^2})^{1/2}h/\tfrac{1}{2}\rho\bar{u}_h^3 \tag{13}$$

The measured values for these coefficients are given in Table 1. The cross-correlation matrices $[r]$ and $[\dot{r}]$, as defined in Sections 2.1 and 2.2, were also measured and these are shown in Table 2. As both matrices are symmetric with all the diagonal elements equal to unity, they are shown as a single matrix with the upper triangle containing the r_{ij} terms, and the lower triangle, the $\dot{r}_{ij}$ values.

TABLE 1

Basic panel pressure coefficients for a single-storey house

Panel no.	$\overline{C_p}$	C_p'	$\hat{C}_p$	$\check{C}_p$	$(h/u_h)\dot{C}_p'$
1	0.55	0.22	1.55	−0.05	0.11
2	0.66	0.28	2.08	−0.08	0.16
3	−1.07	0.33	0.03	−2.74	0.23
4	−0.47	0.16	0.01	−1.36	0.12
5	−0.54	0.15	−0.17	−1.28	0.10
6	−0.60	0.17	−0.18	−1.33	0.08
7	−0.32	0.10	−0.02	−0.87	0.07
8	−0.20	0.07	0.09	−0.62	0.07
9	−0.12	0.07	0.13	−0.49	0.06
10	−0.11	0.05	0.11	−0.39	0.04

TABLE 2

$[r]$ and $[\dot{r}]$ matrices for a single-storey house: $[r]$, top right; $[\dot{r}]$, bottom left (both matrices symmetrical about diagonal with elements equal to unity)

	1	2	3	4	5	6	7	8	9	10
1	1.0	0.95	−0.61	−0.18	−0.47	−0.54	−0.32	−0.12	0.02	0.00
2	0.76	1.0	−0.63	−0.14	−0.48	−0.55	−0.38	−0.18	−0.07	−0.03
3	−0.43	−0.48	1.0	0.69	0.78	0.73	0.70	0.57	0.47	0.45
4	0.01	0.00	0.12	1.0	0.66	0.51	0.63	0.62	0.53	0.55
5	0.03	0.01	0.25	−0.09	1.0	0.95	0.90	0.74	0.57	0.55
6	0.01	0.01	0.16	0.10	0.13	1.0	0.92	0.73	0.55	0.56
7	0.06	0.03	0.14	0.15	0.16	0.31	1.0	0.90	0.76	0.74
8	0.07	0.06	0.10	0.15	0.19	0.28	0.37	1.0	0.89	0.88
9	0.11	0.06	0.12	0.18	0.22	0.37	0.39	0.42	1.0	0.98
10	0.08	0.05	0.11	0.16	0.19	0.35	0.36	0.39	0.72	1.0

Note that the correlation coefficients for the derivatives, $\dot{r}_{ij}$, are considerably lower in magnitude than those for the pressure fluctuations themselves, r_{ij}; this reflects the higher frequency-content of derivatives. Negative correlations occur between the pressures at the windward wall and the roof; this is to be expected, as the roof pressure will tend to fall (suction increases) as the windward-wall pressure increases. Another interesting feature is that the observed correlation coefficients between the roof panel 3 and panels 5, 6 and 7, are higher than that between panels 3 and 4. This has been observed previously by Stathopoulos et al. [11] for a flat roof, and is related to the reattachment of flow onto the roof.

4. Calculation of structural effects

Using the procedure described in Section 2, and the aerodynamic data for the centre bay of the house from Section 3, fluctuating and peak values have

been calculated for a number of overall loads and load effects. These parameters consist of the total lift, drag and overturning moment acting on the section, together with the hold-down forces for the roof trusses supporting the roof bay. Table 3 gives the influence-coefficient vectors for these parameters, and Fig. 5 shows graphically the influence coefficients for the windward hold-down force V_1. The effect of wind pressure under the eaves has been included by introducing dummy panels 2a and 9a, which are assumed to be acted on by pressures fully correlated with those on the adjacent wall-panels 2 and 9, respectively.

TABLE 3

Influence coefficients

Panel no.	Lift β_L	Drag β_D	Overturning moment β_M	Windward truss force β_{V_1}	Leeward truss force β_{V_2}
1	0	1.000	0.750	0	0
2	0	1.000	2.250	0	0
2a	0.985	−0.174	6.775	1.081	−0.096
3	−0.985	0.174	−6.775	−1.081	0.096
4	−0.985	0.174	−5.271	−0.858	−0.127
5	−0.985	0.174	−3.556	−0.604	−0.381
6	−0.986	−0.174	−3.091	−0.381	−0.604
7	−0.985	−0.174	−1.378	−0.127	−0.858
8	−0.985	−0.174	0.127	0.096	−1.081
9a	0.985	0.174	−0.127	−0.096	1.081
9	0	−1.000	−2.250	0	0
10	0	−1.000	−0.750	0	0

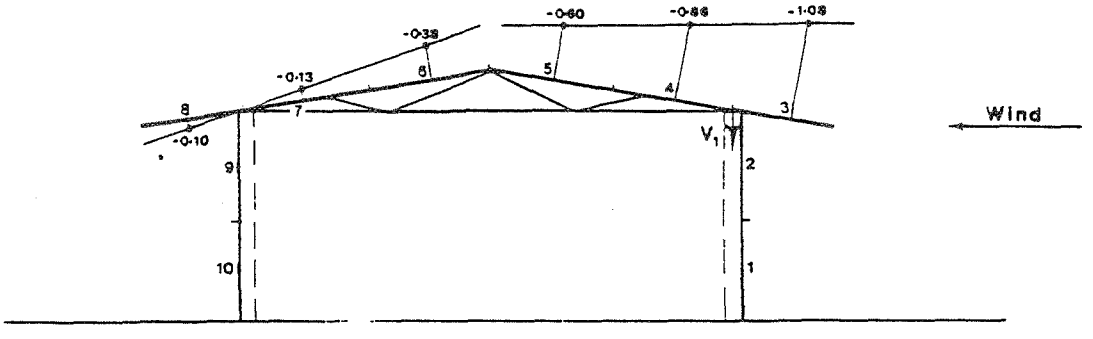

Fig. 5. Influence line for windward truss hold-down force.

The results of the calculations are summarised in Table 4. The numerical values are applicable to the full-scale house, for which the bay width is 2.5 m, and the mean velocity at eaves height was taken to be 30 m s^{-1}.

The gust factor, representing the ratio of the average peak value in a 10 minute period to the mean, is about 2.0 for all the parameters, except for the drag, for which it has a somewhat higher value.

TABLE 4

Calculation of loads ($\bar{u}_h$ = 30 m s^{-1})

	Lift	Drag	Overturning moment	Windward truss force	Leeward truss force
Mean value (kN or kN m)	7.42	2.40	39.7	5.43	1.99
R.m.s. fluctuating value (kN or kN m)	1.97	0.91	11.0	1.50	0.56
Cycling rate, ν (Hz)	0.60	0.74	0.69	0.70	0.72
Peak factor, g (T = 10 min)	3.60	3.66	3.64	3.64	3.64
Peak value (kN or kN m)	14.5	5.74	79.8	10.9	4.0
Gust factor, G	1.96	2.39	2.00	2.00	2.03

TABLE 5

Gust factors derived by various methods (see text)

Load	Covariance integration (i)	Covariance integration with "full" correlation (ii)	Integration of non-simultaneous peaks[a] (iii)	Integration of non-simultaneous peaks[b] (iv)	G_u[2] (v)
L	1.96	2.17	2.72	2.60	2.75
D	2.39	2.43	4.25	3.17	2.75
M	2.00	2.25	2.74	2.73	2.75
V_1	2.00	2.23	2.71	2.68	2.75
V_2	2.03	2.00	3.28	2.36	2.75

[a] Peak giving largest contribution to effect.
[b] Peak having same sign as mean.

It is interesting to compare these estimates of gust factors with a number of other possible estimates, as given in Table 5. Column (i) in Table 5 is taken from Table 4 and represents the covariance integration estimates. Column (ii) is also derived from covariance integration, but "full" correlation of the panel pressure fluctuations was assumed, as follows. When the mean values of the panel pressures were of the same sign, the corresponding correlation coefficients for both the pressures and their derivatives were assumed to be +1. When the mean pressures were of opposite sign, values of −1 were taken for r_{ij} and $\dot{r}_{ij}$. Thus, column (ii) gives essentially the upper limits of the gust factor to be obtained from covariance integration, although, due to variations

in the sign of the influence coefficients, the estimate of the gust factor for the leeward hold-down force, V_2, obtained from the assumption of "full" correlation, is actually lower than that given in column (i).

A conservative value for the gust factor can also be estimated by integrating the instantaneous peak panel pressures, as listed in Table 1, assuming that they acted simultaneously over the structure. This has been done in columns (iii) and (iv) of Table 5. Allowing for the variation in sign of the influence coefficients for the various loads, either the maximum or minimum peak panel pressure will give the largest contribution. This procedure will give the largest possible peak structural-effects and gust-factors that could be estimated from the aerodynamic data obtained: the results are shown in column (iii). For column (iv), the peak pressure having the same sign as the mean pressure for each panel was assumed, giving somewhat lower, but perhaps physically more "realistic", estimates. It can be shown that the estimates in column (ii) are also obtained by integration of the peaks if each panel pressure variation is assumed to be Gaussian; thus column (ii) can be compared to column (iv). Higher values appear in column (iv) because of the non-Gaussian behaviour of the individual panel pressures.

In Codes and Standards based on peak-gust design wind-speeds, design loads are generally obtained by using the design peak-gust wind-speed with mean pressure coefficients. It can be readily shown (e.g., ref. 12) that this inherently assumes a gust factor equal to the square of the gust factor for velocity, G_u. In the case of rural terrain, for the eaves height of the house considered here, the resulting gust factor for loads and their effects is close to 2.75. Thus a constant value of 2.75 appears for all loads in column (v) of Table 5. This approach implies that all pressure fluctuations on the building surface faithfully follow the variations in upwind velocity, in proportion to the square of the velocity. This is some way from the truth for the separated flow regions, however. In fact, the estimates in column (v) are of the same order as those in column (iv), for which non-simultaneous peaks were integrated — an obviously conservative assumption.

Table 5 indicates the reduction in gust factors that can be obtained by using the rational covariance integration approach, compared with simpler, but more conservative and unrealistic, methods. Presumably, even larger reductions can be obtained for effects influenced by larger surface areas of the building, or for larger buildings.

5. Conclusions

This paper has discussed a covariance integration method for the determination of fluctuating and peak structural loads and load effects due to wind on low-rise buildings, or on any other structure for which quasi-static structural behaviour can be assumed. The method is based on the statistical properties of the fluctuating wind pressures on panels, which can be obtained fairly easily from boundary-layer wind tunnel tests. Separate aerodynamic data are required for each wind direction considered, however.

Numerical calculations have been carried out for the central area of a single-storey house, for a mean wind direction normal to one wall of the building. These illustrate the relative ease with which the r.m.s. and peak values of any structural load or effect, for which the influence line is known, can be calculated. Comparison of the calculated peak loads and gust factors with those obtained by integration of non-simultaneous peaks, and with those inherent in Codes and Standards based on peak-gust design wind-speeds, indicates reductions of 20—50%. Presumably even larger reductions will occur for larger areas and for larger buildings.

The method, in its present form, assumes a Gaussian probability distribution for the structural effect under consideration, and thus may tend to give unconservative peak values for effects influenced by small areas of building surface. Further investigation is required to determine the convergence of the probability distributions for structural effects as the area of influence increases. However, the advantages of the method, as described in this paper, justify further development to circumvent the above problem.

6. Acknowledgements

The research work described in this paper was funded by the Australian Housing Research Council. The authors gratefully acknowledge the direct assistance of Mr. G. McNealy, Mr. G. Blakey and Mr. C. Pyne, and useful discussions with Dr. R. Leicester of C.S.I.R.O., Melbourne.

References

1 Standards Association of Australia, S.A.A. Loading Code. Part 2: Wind Forces, AS1170, Part 2, 1975.
2 British Standards Institution, Code of Basic Data for the Design of Buildings. Chapter V: Loading, Part 2: Wind Loads, CP3, Ch. V, Part 2, 1972.
3 A.G. Davenport, D. Surry and T. Stathopoulos, Wind loading on low-rise buildings: final report on phases I and II, University of Western Ontario, Eng. Sci. Res. Rep., BLWT-SS8-1977, 1977.
4 A.G. Davenport, D. Surry and T. Stathopoulos, Wind loading on low-rise buildings: final report on phase III, University of Western Ontario, Eng. Sci. Res. Rep., BLWT-SS4-1978, 1978.
5 D.E. Cartwright and M.S. Longuet-Higgins, The statistical distribution of the maxima of a random function, Proc. R. Soc. London, Ser. A, 237 (1956) 212—232.
6 A.G. Davenport, Note on the distribution of the largest value of a random function with application to gust loading, Proc. I.C.E., 28 (1964) 187—196.
7 J.D. Holmes, Design and performance of a wind tunnel for modelling the atmospheric boundary layer in strong winds, James Cook University of North Queensland, Wind Eng. Rep., 2/77, 1977.
8 T. Stathopoulos, Technique of pneumatically averaging pressures, University of Western Ontario, Eng. Sci. Res. Rep., BLWT-2-1975, 1975.
9 D. Surry and T. Stathopoulos, An experimental approach to the economical measurement of spatially-averaged wind loads, J. Ind. Aerodyn., 2 (1978) 385—397.

10 Engineering Sciences Data Unit, Characteristics of Atmospheric Turbulence Near the Ground. Part II: Single Point Data for Strong Winds (Neutral Atmosphere), Data Item 74031, 1974.
11 T. Stathopoulos, A.G. Davenport and D. Surry, The assessment of effective wind loads acting on flat roofs, Proc. 3rd Colloq. on Industrial Aerodynamics, Aachen, 1978, pp. 225–239.
12 J.D. Holmes, Recent developments in wind loading research and its application to North Australia, Ann. Eng. Conf., I.E. Aust., Townsville, 1976.

Appendix

Consider first the pressure distribution on the various exposed surfaces of a building as represented by a set of discrete pressures, each associated with a tributary area. Each pressure can be represented as the sum of a mean and a fluctuating part:

$P_i = \bar{p}_i + p'_i$, at point i

Assume also that there is an influence coefficient β_i for a particular structural parameter η, associated with the point i: i.e., β_i is the value of structural parameter η when a unit load is applied at the point i. Then the total instantaneous value of η at any point in time is

$$\begin{aligned}\eta &= (\bar{p}_1 + p'_1)\beta_1 \Delta A_1 + (\bar{p}_2 + p'_2)\beta_2 \Delta A_2 + \ldots \\ &= \sum_i (\bar{p}_i + p'_i)\beta_i \Delta A_i \\ &= \sum_i \bar{p}_i\beta_i \Delta A_i + \sum_i p'_i\beta_i \Delta A_i \\ &= \bar{\eta} + \eta'\end{aligned}$$

where $\bar{\eta}$, η' are respectively the mean and fluctuating components of the structural parameter η.
Then

$$\begin{aligned}\eta'^2 &= (p'_1\beta_1 \Delta A_1 + p'_2\beta_2 \Delta A_2 + \ldots)^2 \\ &= p'^2_1\beta^2_1 \Delta A^2_1 + p'^2_2\beta^2_2 \Delta A^2_2 + \ldots + p'_1p'_2\beta_1\beta_2 \Delta A_1 \Delta A_2 + \\ &\quad + p'_1p'_3\beta_1\beta_3 \Delta A_1 \Delta A_3 + \ldots \\ &= \sum_i \sum_j p'_ip'_j\beta_i\beta_j \Delta A_i \Delta A_j\end{aligned}$$

The mean-square fluctuating value is

$$\overline{\eta'^2} = \sum_i \sum_j \overline{p'_ip'_j}\,\beta_i\beta_j \Delta A_i \Delta A_j$$

and the root-mean-square fluctuating value is thus

$$(\overline{\eta'^2})^{1/2} = \left(\sum_i \sum_j \overline{p'_ip'_j}\,\beta_i\beta_j \Delta A_i \Delta A_j\right)^{1/2}$$